JOURNAL OF MATERIALS SCIENCE 29 (1994) 1825–1832

Production of flaky amorphous powders in Fe–Zr–B system by a supercooled liquid quenching method, and their magnetic properties

M. OGUCHI, Y. HARAKAWA
Research and Development, Teikoku Piston Ring Co. Ltd, Okaya 394, Japan
A. INOUE, T. MASUMOTO
Institute for Materials Research, Tohoku University, Sendai 980, Japan
K. SUZUKI
Materials Research Division, Alps Electric Co. Ltd, Nagaoka 940, Japan

By using a supercooled liquid (two-stage) quenching method, in which supercooled liquid droplets produced by high-pressure gas atomization are flattened at high kinetic energies on a rapidly rotating wheel, flaky amorphous powders with a thickness of 1–3 μm and a large aspect ratio of 20–300 were produced for an $Fe_{85}Zr_8B_6Cu_1$ alloy. This is in contrast to the result that spherical powders produced only by high-pressure gas atomization consist of amorphous, b c c and compound, even in the particle size range below 25 μm. The amorphous powder changes to a mostly single b c c phase by annealing for 3.6 ks at 873 K, and the further rise in annealing temperature causes the mixed structure of α-Fe + Fe_3(Zr,B). The annealed flaky powders with the b c c phase exhibit soft magnetic properties of 140 emu g^{-1} for saturation magnetization σ_{10k} and 0.6 Oe for coercivity, H_c. The composite made from the b c c flaky powders and phenol resin at a weight ratio of 9:1 has a high degree of laminated structure. The composite also exhibits soft magnetic properties of 5.3 kG for B_{100}, 150 for μ_{max} and 1.1 Oe for H_c. The B_{100} value is 2.1 times as high as that for the composite of amorphous Co–Fe–Si–B flaky powders and resin. Thus the present composite is expected to be used in applications which require both high saturation magnetization and soft magnetic properties, which cannot be obtained for the composites made from amorphous Co- and Fe-based flaky powders.

1. Introduction

Amorphous alloy powders with spherical, flaky and lump morphologies have been produced by various rapid solidification methods such as gas atomization, roller cavitation and water atomization. The diameter or thickness of amorphous powders produced by these methods is usually larger than 10 μm [1]. No definite technique has been obtained for the production of flaky powders with a small thickness below 5 μm and a large aspect ratio directly from melt, although a ball milling treatment [2] of atomized spherical powders has been used to produce flaky powders with a thickness below 5 μm. Recently, the present authors have succeeded in producing flaky powders with a small thickness of about 1–3 μm through the development of a supercooled liquid (or two-stage) quenching technique [3, 4] in which the supercooled liquid droplets with high-flight velocities produced by high-pressure gas atomization collided and were flattened on the rapidly rotating wheel, which was set just below the atomization nozzle. In addition to the extremely small thickness, it has been clarified [4–6] that the thin flaky powder is solidified at a very high cooling rate which cannot be achieved only by the conventional gas atomization technique. It has further been pointed out that the high cooling rate is due to the combination of small powder thickness, the second-stage cooling of the supercooled liquid droplets and a high thermal conductive state between powder and cooling rotator, resulting from the collision of the supercooled liquid droplets at high kinetic energies.

By utilizing the small thickness and large aspect ratio of the resulting flaky powders, the composite made from the flaky powders and phenol resin is expected to exhibit unique characteristics which are different from those for the powder itself, as well as the melt-spun ribbon with the same alloy composition. More recently, Suzuki *et al.* [7] have reported that a nanoscale b c c structure obtained by crystallization of Fe–Zr–B amorphous alloys exhibits good soft magnetic properties, having simultaneously high saturation magnetization and high permeability. Consequently, if we can produce thin flaky amorphous powders in the Fe–Zr–B system and obtain the

0022–2461 © *1994 Chapman & Hall*

nanoscale bcc structure, the composite consisting of the nanoscale bcc flaky powder embedded in a resin matrix is expected to exhibit good soft magnetic properties with high saturation magnetization, which cannot be obtained in the use of flaky amorphous powders in Co–Fe–Si–B and Fe–Si–B systems. This paper presents the production of flaky Fe–Zr–B amorphous powders and the changes in the structure and soft magnetic properties of the flaky powders by annealing treatment, as well as the magnetic characteristics of the composite materials made from the annealed flaky powders and resin.

2. Experimental procedure

An alloy of nominal composition $Fe_{85}Zr_8B_6Cu_1$ (at %) was used in the present study. A mixture of pure metals and pure crystal boron was melted in an argon atmosphere in an induction furnace and chill-cast in a copper mould to prepare the master alloy. About 500 g of the alloy was charged into the atomization crucible and remelted under an argon atmosphere. The high-pressure gas atomization equipment combined with centrifugal spinning is shown in Fig. 1. This equipment produces flaky powders by first forming spherical liquid droplets by high-pressure argon atomization with a dynamic pressure of 9.8 MPa, followed by impact flattening of the liquid droplets using a revolving substrate. The use of a rotator is essential in the production of flaky powders with high aspect ratio and small thickness. The cone-shaped rotator was made from copper coated with an electrodeposited chromium layer, and had a maximum diameter and height of 200 and 70 mm, respectively. The speed of rotation was fixed at 7200 r.p.m. For comparison, spherical powders were also produced by a conventional high-pressure gas atomization technique. The

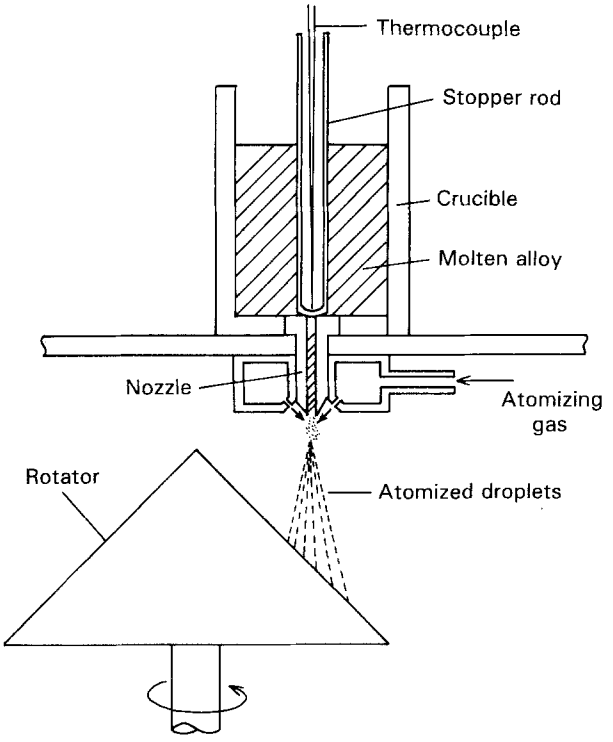

Figure 1 Schematic illustration of two-stage quenching equipment incorporating high-pressure gas atomization and centrifugal spinning.

size distribution of the atomized powders was evaluated by sieving. In addition, the flaky amorphous powders were annealed for 3.6 ks in the temperature range of 750–900 K in an argon atmosphere, with the aim of obtaining a mostly single bcc phase. The structure and morphology of the as-atomized and annealed powders as a function of particle size fraction were examined by X-ray diffractometry (XRD) and scanning electron and optical microscopy (SEM and OM). The magnetic properties of the flaky powders with different size fractions were measured at room temperature under a maximum applied field of 10 kOe with a vibrating sample magnetometer.

The production of composite cores was carried out by the mixing of the sieved powders and phenol resin at a mixing weight ratio of 9:1 (a volume ratio of 59:41), followed by pressing the mixture for 600 s at 423 K under a uniaxial applied load of 13.7 MPa. The resulting composite cores have a disc shape with a height of 5 mm and inner and outer diameters of 18 and 31.5 mm. The d.c. and a.c. magnetic characteristics were measured at room temperature with a *B–H* loop tracer under an applied field of 100 Oe for the former characteristics, 2 Oe in a frequency range of 1 to 100 kHz for the latter.

3. Results and discussion

3.1. Production and properties of flaky amorphous powders

Fig. 2 shows the XRD pattern and morphology of $Fe_{85}Zr_8B_6Cu_1$ powders produced by high-pressure gas atomization. Some diffraction peaks corresponding to compounds are seen on the broad peak due to the formation of the amorphous phase, indicating that no amorphous single phase is formed even in the particle size fraction below 25 μm. It is thus concluded that the cooling rate achieved only by the high-pressure gas atomization technique is not high enough to produce an amorphous single phase. It has further been clarified [7] that good, soft magnetic properties are not obtained from the amorphous phase including compounds in any annealing conditions.

Accordingly, possibilities for the formation of an amorphous single phase in Fe–Zr–B alloys were investigated by using the two-stage quenching process. Fig. 3 shows the shape and surface morphology of flaky $Fe_{85}Zr_8B_6Cu_1$ powders produced by the supercooled liquid quenching technique. The powders with a particle size fraction above 25 μm have an oval shape and the surface and edge appear to be very smooth. The thickness is as small as 1–3 μm and the aspect ratio defined by the ratio of larger length to thickness is as large as 20–300. The ratio of longer size to shorter size is measured to be about 1.5. The morphology for the flaky powders is the same as that for other flaky powders in (Fe,Co,Ni)–Si–B [3, 4], Fe–P–C [4] and Al–Ni–Mm [5] systems. Fig. 4 shows the XRD pattern of the flaky $Fe_{85}Zr_8B_6Cu_1$ powders with different particle size fractions. The patterns of the flaky powders consist only of a broad peak in all the particle size fractions of 25–150 μm, indicating the formation of an amorphous single phase. This result is significantly different from the

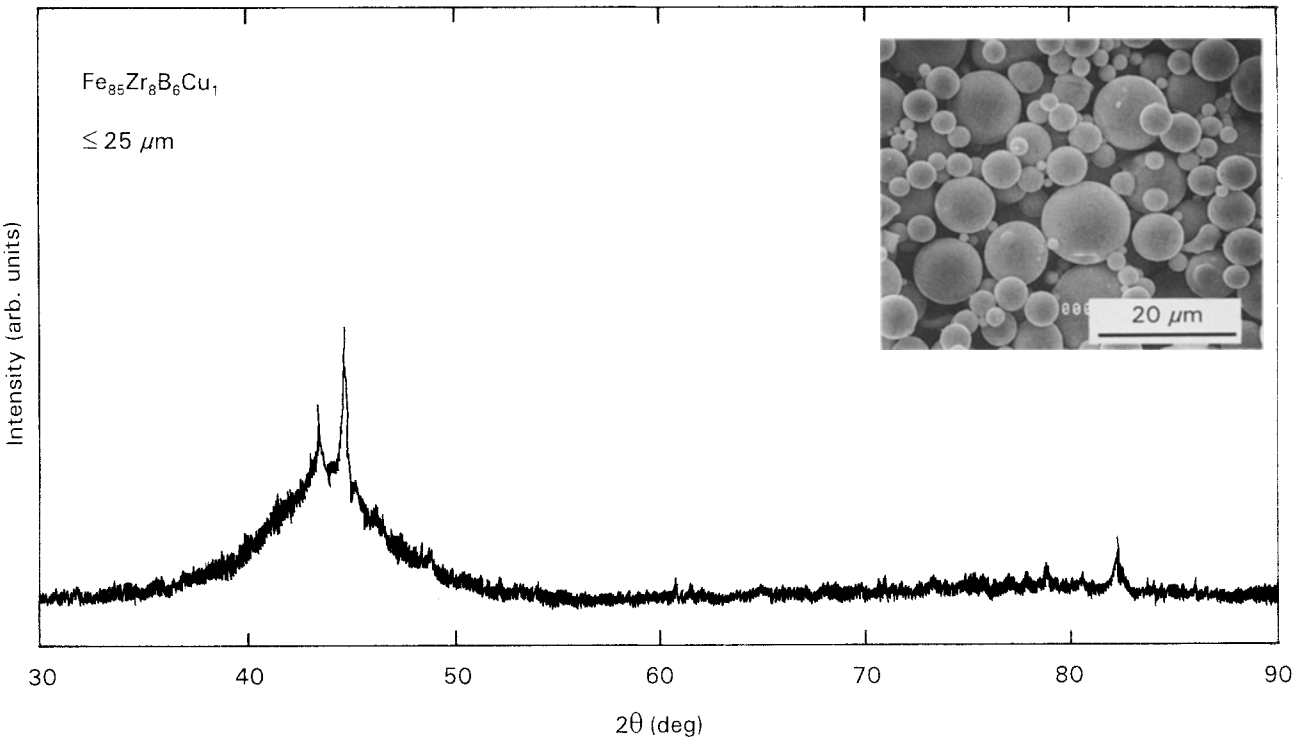

Figure 2 X-ray diffraction pattern and scanning electron micrograph taken from $Fe_{85}Zr_8B_6Cu_1$ powders produced by conventional argon gas atomization technique.

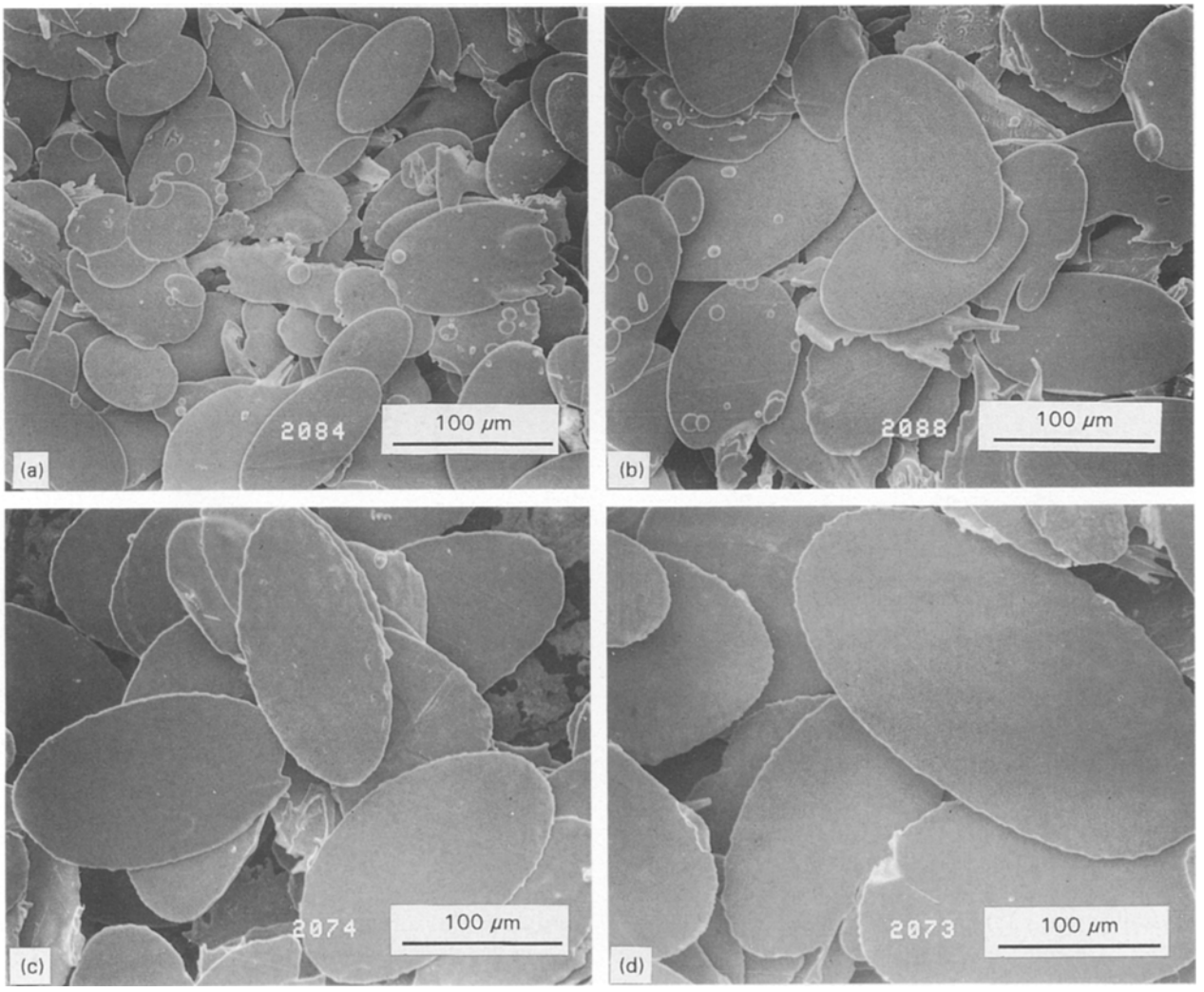

Figure 3 Scanning electron micrographs showing the morphology of $Fe_{85}Zr_8B_6Cu_1$ powders produced by the two-stage quenching method. (a) 25–45; (b) 45–63; (c) 63–90; (d) 90–150 μm.

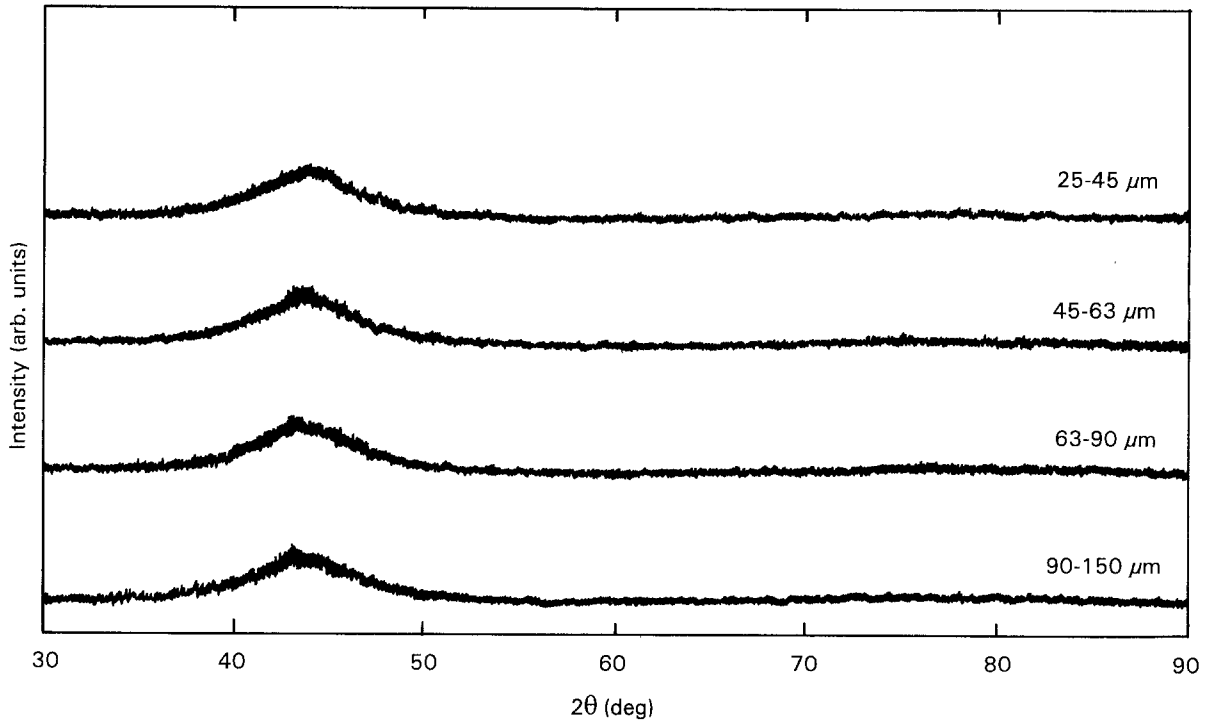

Figure 4 X-ray diffraction patterns showing the influence of particle size fraction on the structure in $Fe_{85}Zr_8B_6Cu_1$ powders produced by the two-stage quenching method.

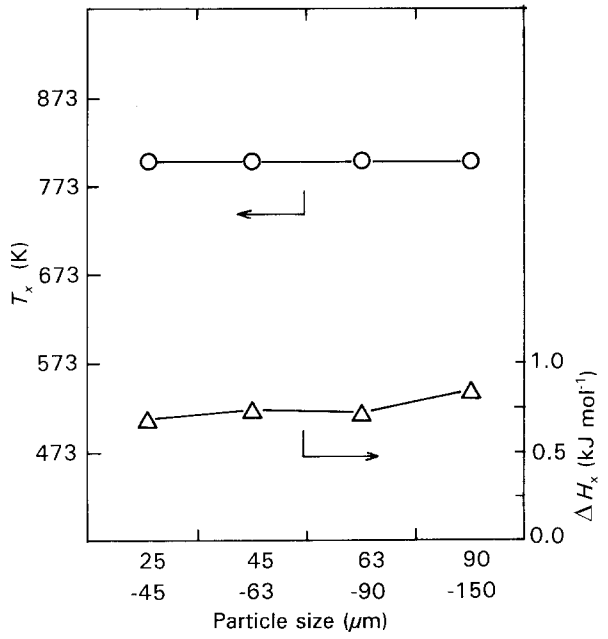

Figure 5 Onset temperature for crystallization (T_x) and heat of crystallization (ΔH_x) as a function of particle size fraction for the amorphous $Fe_{85}Zr_8B_6Cu_1$ powders at 0.67 K s^{-1}.

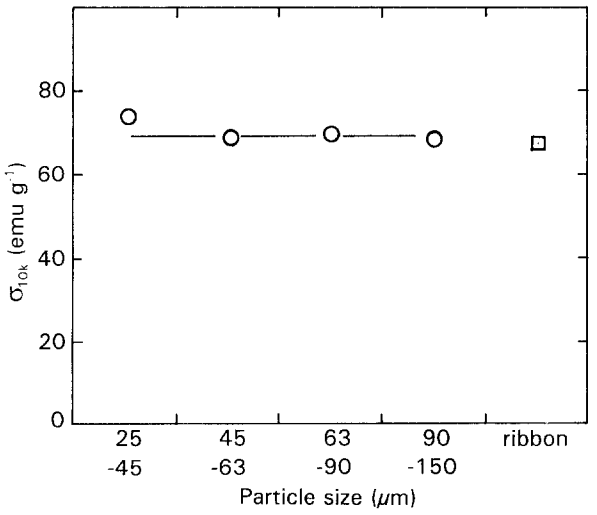

Figure 6 Saturation magnetization (σ_{10k}) as a function of particle size fraction for the amorphous, as-quenched $Fe_{85}Zr_8B_6Cu_1$ powders.

formation of the mixed structure of amorphous and crystalline phases for the spherical powders with a particle size fraction below 25 μm. It is therefore concluded that the cooling rate is much larger for the present two-stage quenching technique than for the single-stage high-pressure gas atomization method.

Fig. 5 shows the changes in the onset temperature of crystallization (T_x) and the heat of crystallization (ΔH_x) as a function of particle size fraction for the Fe–Zr–B–Cu flaky powders. No distinct difference in T_x and ΔH_x with particle size fraction is seen, being consistent with the result obtained by XRD. Fig. 6 shows the saturation magnetization in an applied field of 10 kOe, σ_{10k}, as a function of particle size fraction for the flaky powders. σ_{10k} is about 70 emu g^{-1} over the whole particle size range and agrees with that [7] for the melt-spun amorphous ribbon. The rather low σ_{10k} value in the amorphous state has been thought [7, 8] to originate from the Invar effect.

It has previously been reported [9] that the melt-spun $Fe_{85}Zr_8B_6Cu_1$ amorphous ribbon changes to a mostly single bcc phase with a nanoscale grain size, and the structural change causes a remarkable improvement of soft magnetic properties combined with a significant increase in saturation magnetization. The possibility of similar changes in structure and magnetic properties was examined for the Fe–Zr–B–Cu flaky powders. Fig. 7 shows the change in the XRD

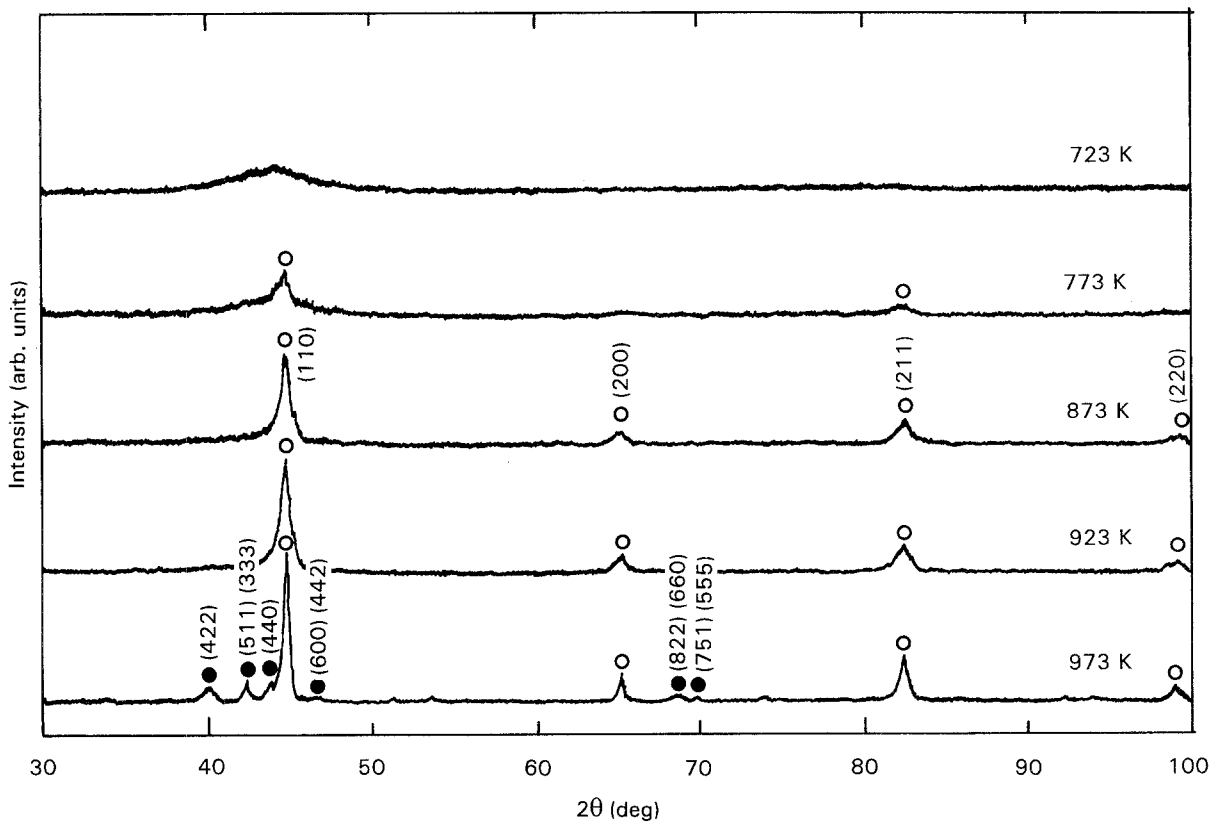

Figure 7 X-ray diffraction patterns for the amorphous $Fe_{85}Zr_8B_6Cu_1$ powders with a particle size fraction of 25–150 μm annealed for 3.6 ks at temperatures between 723 and 973 K. ○, bcc–Fe; ●, Fe_3Zr.

pattern with annealing temperature for 3.6 ks. The amorphous structure remains unchanged at temperatures below 723 K, but the bcc phase begins to precipitate at 773 K, followed by the progress of the transition of the remaining amorphous phase to bcc phase in the temperature range of 873–923 K and then the transition of the bcc phase to α-Fe plus $Fe_3(Zr,B)$. In order to investigate the change in the solute content in the bcc phase with T_a, the lattice parameter of the bcc phase determined from the XRD diffraction patterns is plotted as a function of T_a in Fig. 8. The lattice parameter decreases significantly in the T_a range of 773–873 K, shows a nearly constant value of 0.2867 nm and then increases slightly with further increasing T_a. Considering that the lattice parameter of pure α-Fe is 0.28664 nm [10], it is presumed that the significant decrease in the lattice parameter is due to the decrease in Zr content in the bcc phase, while the slight increase in a_0 results from the decrease in B content in the bcc phase resulting from the precipitation of $Fe_3(Zr,B)$. The previous detailed study [11] on the crystallization behaviour of the Fe–Zr–B amorphous alloys has indicated that the decrease in the solute content in the bcc phase occurs through the movement of the solute elements from the bcc phase to the remaining amorphous phase. Thus the decomposition behaviour of the amorphous flaky powder is the same as that [9, 11] for the melt-spun amorphous ribbon with the same alloy composition, and the crystallization behaviour is independent of the difference in the morphology and thickness of the sample.

Fig. 9 shows the changes in saturation magnetization in a field of 2 kOe (σ_{2k}) and coercivity (H_c) as a

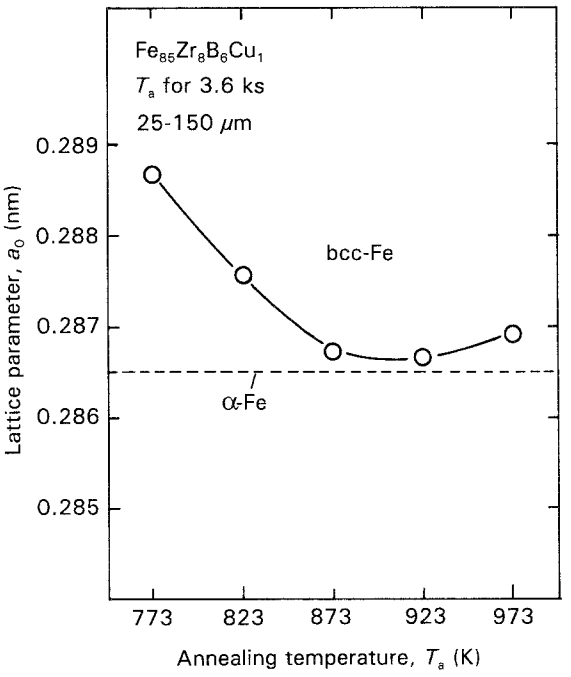

Figure 8 Lattice parameter of the bcc phase obtained by annealing the amorphous $Fe_{85}Zr_8B_6Cu_1$ powder with a particle size fraction of 25–150 μm as a function of annealing temperature. T_a, 3.6 ks.

function of T_a for the $Fe_{85}Zr_8B_6Cu_1$ flaky powders. The transition of amorphous to bcc phase causes a significant increase in σ_{2k} and a decrease in H_c, followed by a rapid increase in H_c by the precipitation of $Fe_3(Zr,B)$. The changes in σ_{2k} and H_c with T_a are in agreement with those [9] for the melt-spun Fe–Zr–B–Cu ribbon. It is thus concluded that the annealing of the flaky amorphous powder for

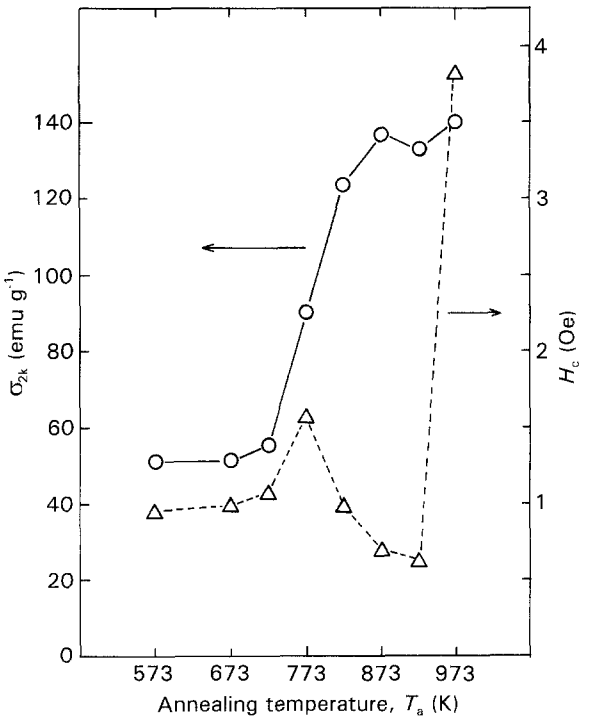

Figure 9 Saturation magnetization (σ_{2k}) and coercivity (H_c) as a function of annealing temperature for the amorphous $Fe_{85}Zr_8B_6Cu_1$ powders with a particle size fraction of 25–150 μm.

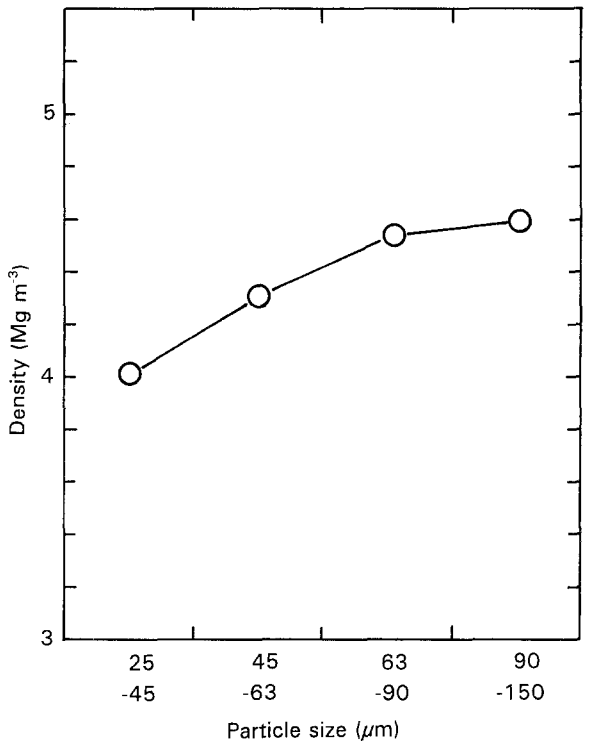

Figure 11 Density of $Fe_{85}Zr_8B_6Cu_1$ composites as a function of particle size fraction, annealed at 873 K for 3.6 ks. $\phi 31.5 \times \phi 18 \times 5$.

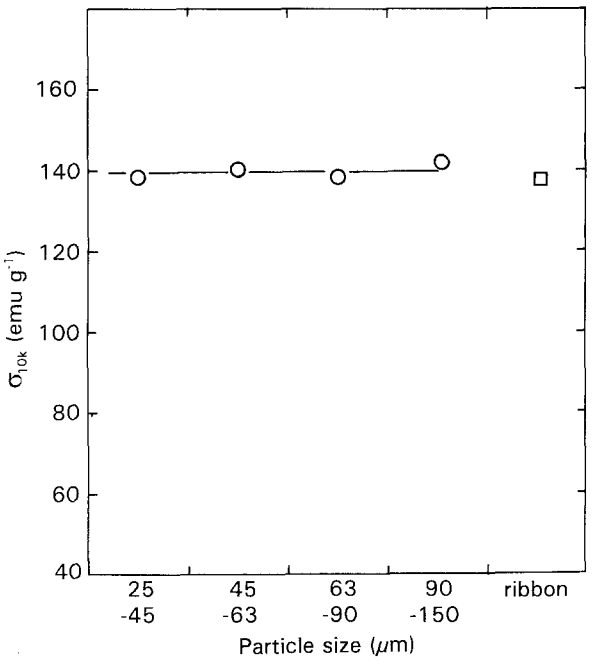

Figure 10 Saturation magnetization (σ_{10k}) as a function of particle size fraction for the bcc $Fe_{85}Zr_8B_6Cu_1$ powders produced by annealing the amorphous powders for 3.6 ks at 873 K.

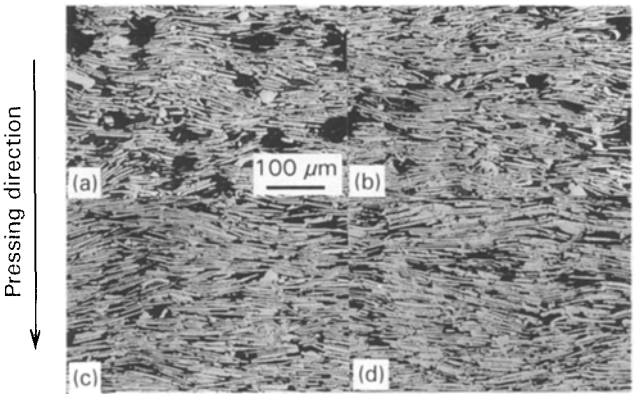

Figure 12 Optical micrographs showing the cross-sectional structure of $Fe_{85}Zr_8B_6Cu_1$ composites made from the bcc powders of phenol resin at a weight ratio of 9:1. (a) 25–45; (b) 45–63; (c) 63–90; (d) 90–150 μm.

3.6 ks at 923 K results in good, soft magnetic properties of 133 emu g^{-1} for σ_{2k} and 0.6 Oe for H_c. Furthermore, it is seen in Fig. 10 that the saturation magnetization for the bcc flaky powder (σ_{10k} = 139 emu g^{-1}), is independent of particle size.

3.2. Magnetic properties of composite cores

Based on the data for the annealing temperature dependence of permeability and coercivity for the amorphous flaky powders, the bcc phase powders obtained by annealing for 3.6 ks at 873 K were used for the production of the composite cores. Fig. 11 shows density as a function of particle size fraction for the $Fe_{85}Zr_8B_6Cu_1$ composite cores. The density increases from 4.0 to 4.6 Mg m^{-3} with increasing particle size fraction, presumably because of an increase in the degree of the leafing effect [12] in which the flaky powders lie spontaneously and densely in a laminating mode in the phenol resin. Fig. 12 shows optical micrographs revealing the cross-sectional structure of the composite cores. As the powder size increases, the directionality of the powders which lie perpendicular to the pressing direction increases, in agreement with the tendency for the density to increase with increasing powder size (or aspect ratio). Fig. 13 shows the d.c. *B–H* curves for the

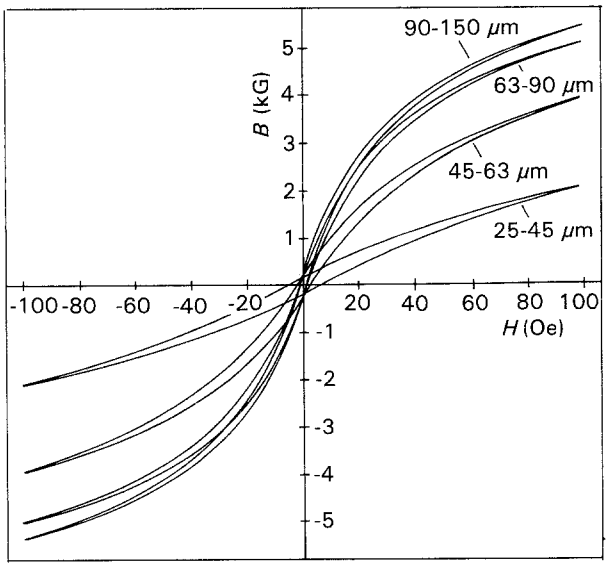

Figure 13 Change in the B–H curve of $Fe_{85}Zr_8B_6Cu_1$ composites with powder size fraction. Annealed at 873 K for 3.6 ks. $\phi 31.5 \times \phi 18 \times 5$.

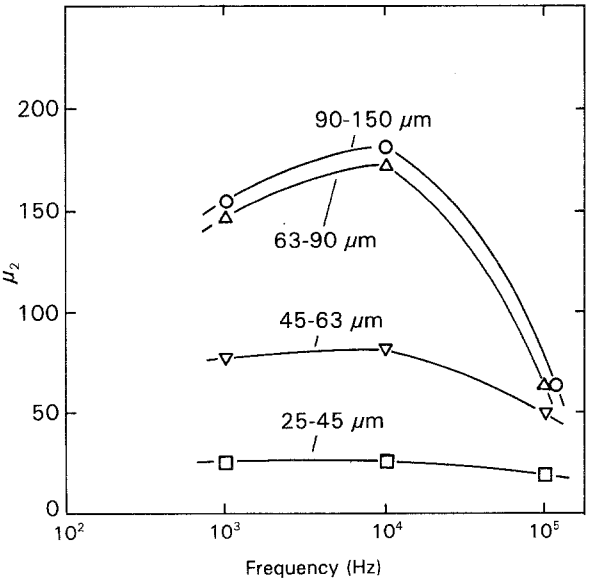

Figure 15 Permeability at a field of 2 Oe (μ_2) as a function of frequency for $Fe_{85}Zr_8B_6Cu_1$ composites made from different powder sizes. Annealed at 873 k for 3.6 ks. $\phi 31.5 \times \phi 18 \times 5$.

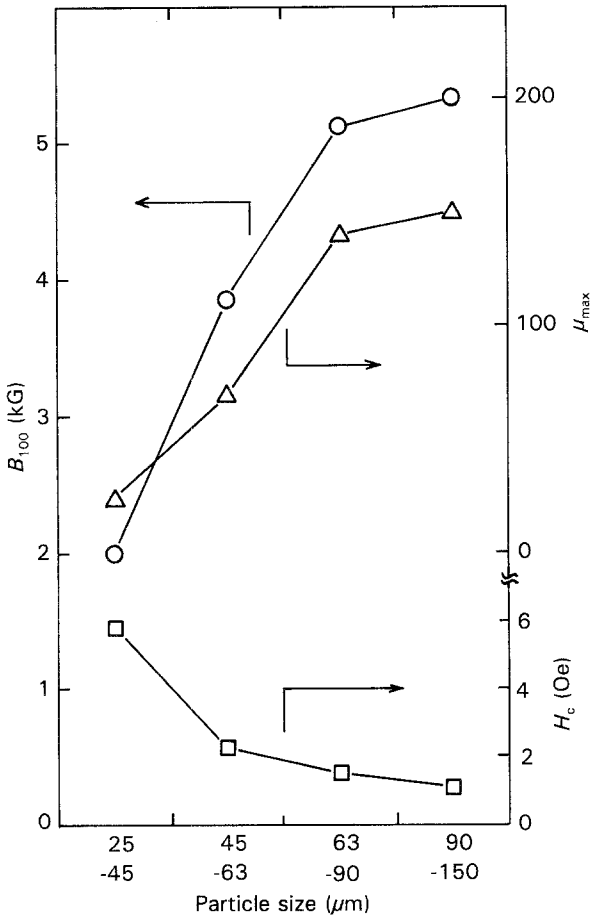

Figure 14 Magnetic flux density (B_{100}), maximum permeability (μ_{max}) and coercive force (H_c) as a function of particle size fraction for $Fe_{85}Zr_8B_6Cu_1$ composites annealed at 873 K for 3.6 ks. $\phi 31.5 \times \phi 18 \times 5$.

$Fe_{85}Zr_8B_6Cu_1$ composite cores. The increase in magnetization in a low applied field becomes significant with increasing powder size, indicating an increase in permeability. Based on the d.c. B–H curves, B_{100}, μ_{max} and H_c are plotted as a function of particle size fraction in Fig. 14. As the particle size increases from 25 to 150 μm, B_{100} and μ_{max} increase from 2.0 to 5.3 kG and from 25 to 150, respectively, while H_c decreases from 5.8 to 1.1 Oe. This particle size dependence is presumably because of an increase in the density of the composite and a decrease in the coefficient of antiferromagnetism resulting from the increase in the directionality of the flaky powders with increasing particle size. The frequency dependence of μ_2 for the composite cores is shown in Fig. 15. μ_2 has larger values for the flaky powders with larger particle size, being consistent with the tendency for the d.c. B–H curves. μ_2 remains almost unchanged in the frequency range up to 10 kHz and decreases significantly in the higher frequency range. The decrease in μ_2 is more significant for the larger powders with larger μ_2. From these results, it is concluded that the composite cores, consisting of the bcc $Fe_{85}Zr_8B_6Cu_1$ flaky powders with a size of 90–150 μm embedded in the phenol resin, exhibit magnetic properties of 5.3 kG for B_{100}, 150 for μ_2 at 10 kHz, and 1.1 Oe for H_c. The B_{100} value is about 2.1 times as high as that [13] for the composite made from $Co_{70.3}Fe_{4.7}Si_{10}B_{15}$ flaky powders and phenol resin at the same weight ratio.

4. Conclusion

By using the supercooled liquid quenching method developed by the present authors, amorphous $Fe_{85}Zr_8B_6Cu_1$ flaky powders with a very small thickness of 1–3 μm, and large aspect ratios of 20–300, were produced directly from the melt. The amorphous structure of the flaky powders changes to a mostly single bcc structure upon annealing for 3.6 ks at 873 K, and the structural change causes the soft magnetic properties of 140 for σ_{2k} and 0.6 Oe for H_c. Furthermore, the composite cores with a height of 5 mm and inner and outer diameters of 18 and 31.5 mm, respectively, were made from the bcc flaky powders obtained by annealing for 3.6 ks at 873 K and phenol resin. The density of the resulting com-

posite core increases with increasing particle size, accompanied by an increase in the tendency for the powders to lie perpendicular to the compressive stress. The resulting composite core containing the bcc powders, with sizes ranging from 90–150 μm, exhibited 5.3 kG for B_{100}, 1.1 Oe for H_c and 154 for μ_2 at 1 kHz. It is notable that the B_{100} value of the composite is much higher than that (2.6 kG) for the composite consisting of Co–Fe–Si–B amorphous powders embedded in resin. Thus, the Fe–Zr–B–Cu composites are very attractive as a magnetic core material in which a high B_s is required.

References

1. S. A. MILLER, "Amorphous Metallic Alloys", edited by F. E. Luborsky (Butterworths, London, 1983) p. 506.
2. J. D. JAMES, B. WILSHIRE and D. CLEAVER, *Powder Metall.* **33** (1990) 247.
3. A. INOUE, T. KOMURA, J. SAIDA, M. OGUCHI, H. M. KIMURA and T. MASUMOTO, *Int. J. Rapid Solidification* **4** (1989) 181.
4. A. INOUE, J. SAIDA, Y. TACHIYA, A. P. TSAI and T. MASUMOTO, *Mater. Res. Soc.* **3** (1989) 359.
5. A. INOUE, M. OGUCHI, H. YAMAGUCHI and T. MASUMOTO, *Mater. Trans. JIM* **30** (1989) 1033.
6. M. OGUCHI, A. INOUE and T. MASUMOTO, *Mater. Sci. Engng* **A133** (1991) 688.
7. K. SUZUKI, N. KATAOKA, A. INOUE, A. MAKINO and T. MASUMOTO, *Mater. Trans. JIM* **31** (1990) 743.
8. S. OHNUMA, M. NOSE, K. SHIRAKAWA and T. MASUMOTO, *Sci. Rep. Res. Inst. Tohoku Univ.* **A29** (1981) 254.
9. K. SUZUKI, A. MAKINO, N. KATAOKA, A. INOUE and T. MASUMOTO, *Mater. Trans. JIM* **32** (1991) 93.
10. W. B. PEARSON, "A Handbook of Lattice Spacings and Structures of Metals and Alloys" (Pergamon, Oxford, 1964) p. 625.
11. K. SUZUKI, M. KIKUCHI, A. MAKINO, A. INOUE and T. MASUMOTO, *Mater. Trans. JIM* **32** (1991) 961.
12. O. IWAO and Y. HASHIZUME, *J. Jpn Inst. Light Metals* **32** (1982) 622.
13. M. OGUCHI, Y. HARAKAWA, Y. SHIMIZU, A. INOUE and T. MASUMOTO, *Powder Powder Metall.* **38** (1991) 930.

Received 19 February
and accepted 6 October 1993